

# Fluorescent 1,10-Phenanthroline-Containing Oligonucleotides Distinguish between Perfect and Mismatched Base Pairing

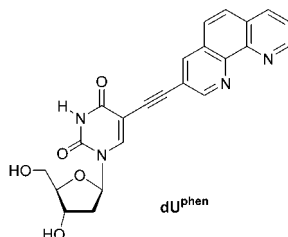
Dennis J. Hurley, Susan E. Seaman, Jan C. Mazura, and Yitzhak Tor\*

Department of Chemistry and Biochemistry, University of California, San Diego,  
La Jolla, California 92093-0358

ytor@ucsd.edu

Received April 18, 2002

## ABSTRACT



A fluorescent deoxyuridine analogue is sensitive to the polarity of its environment and exhibits a distinct emission profile in single- vs double-stranded oligonucleotides. Emission-monitored denaturation curves of internally modified  $dU^{\text{phen}}$  duplexes are characteristic of the base opposite  $dU^{\text{phen}}$  and distinguish between perfect and mismatched complementary oligonucleotides.

Fluorescent nucleosides that are sensitive to the local environment within DNA duplexes have been attracting attention as probes for DNA hybridization and DNA–ligand interactions.<sup>1</sup> Various approaches have been explored, including the following: (a) isomorphous base analogues such as 2-aminopurine<sup>2</sup> and 5-methylpyrimidin-2-one,<sup>3</sup> (b) extended bases such as 1,*N*<sup>6</sup>-ethenoadenine<sup>4</sup> and benzo[*g*]-

quinazoline-2,4-(1*H*,3*H*)-dione,<sup>5</sup> (c) base conjugates such as pyrene-linked pyrimidines<sup>6</sup> or ethynyl extended deazapurines,<sup>7</sup> and (d) nucleoside analogues with fluorophores replacing the natural heterocycles.<sup>8</sup> Such modifications are particularly valuable since the natural bases are practically nonemissive<sup>9</sup> and end labeling with fluorescent tags is not necessarily sensitive to remote binding events. No universal

(1) For review articles, see: Wojcieszki, C.; Stolze, K.; Engels, J. W. *Synlett* **1999**, 1667–1678. Hawkins, M. E. *Cell Biochem. Biophys.* **2001**, *34*, 257–281.

(2) For selected examples, see: Ward, D. C.; Reich, E.; Stryer, L. J. *Biol. Chem.* **1969**, *244*, 1228–1237. Menger, M.; Tuschl, T.; Eckstein, F.; Porschke, D. *Biochemistry* **1996**, *35*, 14710–14716. Lacourciere, K. A.; Stivers, J. T.; Marino, J. P. *Biochemistry* **2000**, *39*, 5630–5641. Kawai, M.; Lee, M. J.; Evans, K. O.; Nordlund, T. M. *J. Fluoresc.* **2001**, *11*, 23–32. Jean, J. M.; Hall, K. B. *Proc. Natl. Acad. Sci. U.S.A.* **2001**, *98*, 37–41. Rachofsky, E. L.; Osman, R.; Ross, J. B. A. *Biochemistry* **2001**, *40*, 946–956. Kirk, S. R.; Luedtke, N. W.; Tor, Y. *Bioorg. Med. Chem.* **2001**, *9*, 2295–2301.

(3) Singleton, S. F.; Shan, F.; Kanan, M. W.; McIntosh, C. M.; Stearman, C. J.; Helm, J. S.; Webb, K. J. *Org. Lett.* **2001**, *3*, 3919–3922.

(4) Secrist, J. A., III; Barrio, J. R.; Leonard, N. J. *Science* **1972**, *175*, 646–647. Holmén, A.; Albinsson, Nordén, B. *J. Phys. Chem.* **1994**, *98*, 13460–13469 and references therein.

(5) Godde, F.; Toulmé, J.-J.; Moreau, S. *Biochemistry* **1998**, *37*, 13765–13775. Arzumanov, A.; Godde, F.; Moreau, S.; Toulmé, J.-J.; Weeds, A.; Gait, M. J. *Helv. Chim. Acta* **2000**, *83*, 1424–1436.

(6) Netzel, T. L.; Zhao, M.; Nafisik, K.; Headrick, J.; Sigman, M. S.; Eaton, B. E. *J. Am. Chem. Soc.* **1995**, *117*, 9119–9128. Manoharan, M.; Tivel, K. L.; Zhao, M.; Nafisil, K.; Netzel, T. L. *J. Phys. Chem.* **1995**, *99*, 17461–17472. Kerr, C. E.; Mitchell, C. D.; Headrick, J.; Eaton, B. E.; Netzel, T. L. *J. Phys. Chem. B* **2000**, *104*, 1637–1650.

(7) Seela, F.; Zulauf, M.; Sauer, M.; Deimel, M. *Helv. Chim. Acta* **2000**, *83*, 910–927. Seela, F.; Feiling, E.; Gross, J.; Hillenkamp, F.; Ramzaeva, N.; Rosemeyer, H.; Zulauf, M. *J. Biotech.* **2001**, *86*, 269–279.

(8) Paris, P. L.; Langenhan, J. M.; Kool, E. T. *Nucleic Acids Res.* **1998**, *26*, 3789–3793. Strässler, C.; Davis, N. E.; Kool, E. T. *Helv. Chim. Acta* **1999**, *82*, 2160–2171. Singh, I.; Hecker, W.; Prasad, A. K.; Parmar, V. S.; Seitz, O. *Chem. Commun.* **2002**, 500–501.

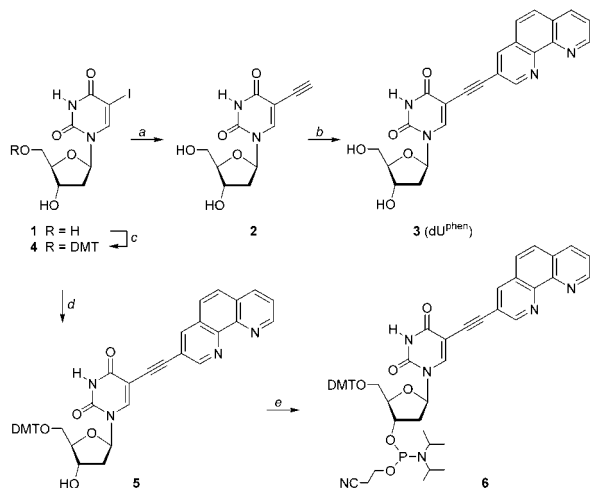
(9) Daniels, M.; Hauswirth, W. *Science* **1971**, *171*, 675–677. Pecourt, J.-M. L.; Peon, J.; Kohler, B. *J. Am. Chem. Soc.* **2000**, *122*, 9348–9349.

solutions exist, however, and additional modifications have to be developed and empirically evaluated.

We have previously demonstrated that extending the conjugation of 1,10-phenanthroline via ethynyl linkages provides a unique family of intense and tunable fluorophores, where changes in the electronic polarization, solvation, and coordination are translated into dramatic spectral changes.<sup>10</sup> These observations have prompted us to explore conjugated 1,10-phenanthroline-containing nucleosides as “reporter” probes for the local environment of the DNA double helix. Here, we disclose the synthesis of a novel fluorescent nucleoside and its incorporation into oligonucleotides using solid-phase phosphoramidite chemistry. The emission of the fluorescent DNA oligonucleotides changes upon hybridization, and is sensitive to the formation of a Watson–Crick vs mismatched base pairing.

The building block for synthesizing fluorescent oligonucleotides is a modified 2'-deoxyuridine **3** (dU<sup>phen</sup>), where the 5-position on the heterocyclic base is conjugated to a 1,10-phenanthroline at the 3 position via an ethynyl linker (Scheme 1). Its synthesis entails the preparation of 5-eth-

**Scheme 1.** Synthesis of dU<sup>phen</sup> **3** and Its Phosphoramidite **6**<sup>a</sup>



<sup>a</sup> Reagents and conditions: (a) (i) (CF<sub>3</sub>CO)<sub>2</sub>O; (ii) Me<sub>3</sub>SiC≡CH, (Ph<sub>3</sub>P)<sub>4</sub>Pd, CuI, DMF, Et<sub>3</sub>N, 95–98%; (iii) K<sub>2</sub>CO<sub>3</sub>, MeOH, 75–92%; (b) 3-bromo-1,10-phenanthroline, (dppf)PdCl<sub>2</sub>·CH<sub>2</sub>Cl<sub>2</sub>, CuI, DMF, Et<sub>3</sub>N, 72–84%; (c) 4,4'-dimethoxytrityl chloride (DMT-Cl), DMAP, pyridine, Et<sub>3</sub>N, 92%; (d) 3-ethynyl-1,10-phenanthroline, (dppf)PdCl<sub>2</sub>·CH<sub>2</sub>Cl<sub>2</sub>, CuI, DMF, Et<sub>3</sub>N, 73–76%; (e) (*i*-Pr<sub>2</sub>N)<sub>2</sub>-POCH<sub>2</sub>CH<sub>2</sub>CN, 1*H*-tetrazole, CH<sub>3</sub>CN, 81%.

nyl-2'-deoxyuridine **2**, a known modified nucleoside obtained from the commercially available 5-iodo-2'-deoxyuridine **1**,<sup>11</sup> followed by a palladium-catalyzed cross-coupling reaction with 3-bromo-1,10-phenanthroline<sup>12</sup> (Scheme 1). Alternatively, treating 5-iodo-2'-deoxyuridine **1** with 4,4'-dimethoxy-

trityl chloride in the presence of 4-(dimethylamino)pyridine provides the DMT-protected nucleoside **4**, which is cross-coupled to 3-ethynyl-1,10-phenanthroline to give **5**. Phosphitylation with (2-cyanoethoxy)-bis(diisopropyl-amino)-phosphine in the presence of 1*H*-tetrazole yields the corresponding phosphoramidite **6**.<sup>13</sup>

Phenanthroline-containing oligonucleotides, incorporating the modified base dU<sup>phen</sup> at various positions, have been prepared in good yields using the novel phosphoramidite **6**.<sup>14</sup> Figure 1 shows the various oligonucleotides used in this

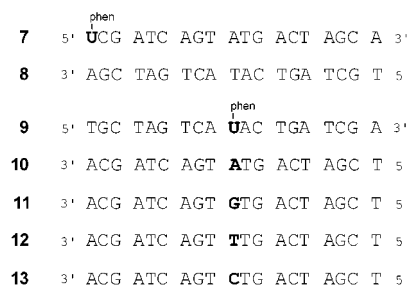


**Figure 1.** Oligonucleotides synthesized and studied.

study. The incorporation of a phenanthroline-containing nucleoside has a relatively small detrimental effect on duplex stability as determined by thermal denaturation measurements.<sup>13</sup>

Figure 2 shows the normalized absorption and emission

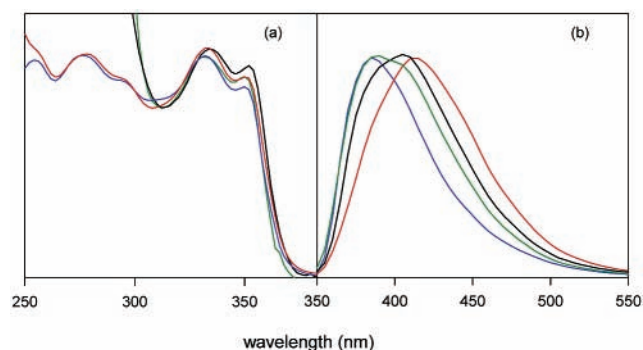


**Figure 2.** Normalized absorption (a) and emission (b) spectra of dU<sup>phen</sup> in CH<sub>2</sub>Cl<sub>2</sub> (blue) or phosphate buffer (red), single stranded oligo **9** (black) and duplex **9**·**10** in aqueous buffer (green).

spectra of the dU<sup>phen</sup> nucleoside **3** in dichloromethane and in water. While the absorption spectra show little sensitivity to solvent polarity, the emission maxima are much more susceptible to environmental changes. Upon excitation at 333

(10) Joshi, H. S.; Jamshidi, R.; Tor, Y. *Angew. Chem., Int. Ed.* **1999**, *38*, 2721–2725.

(11) Robins, M. J.; Barr, P. J. *J. Org. Chem.* **1983**, *48*, 1854–1862. Hashimoto, H.; Nelson, M. G.; Switzer, C. J. *Am. Chem. Soc.* **1993**, *115*, 7128–7138.

(12) Tzalis, D.; Tor, Y.; Failla, S.; Siegel, J. S. *Tetrahedron Lett.* **1995**, *36*, 3489–3490. Tzalis, D.; Tor, Y. *Tetrahedron Lett.* **1995**, *36*, 6017–6020. Connors, P. J., Jr.; Tzalis, D.; Dunnick, A. L.; Tor, Y. *Inorg. Chem.* **1998**, *37*, 1121–1123.

(13) See the Supporting Information for additional experimental details.

nm of a dilute solution in dichloromethane, nucleoside **3** displays an intense purple emission that peaks at 385 nm and extends into the visible range. In water, on the other hand, the emission spectrum displays a maximum at 408 nm. As shown in Figure 3, this tendency holds for a number of

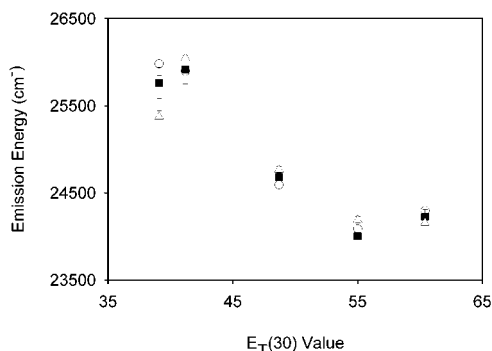


**Figure 3.** Emission energy vs  $E_T(30)$  value for dU<sup>phen</sup> **3** (square), O-Me **14** (triangle), and N-Me **15** (circle).

solvents, where decreasing solvent polarity results in higher emission energy. The bathochromic shift observed upon increasing solvent polarity is suggestive of a greater stabilization of the excited state. This trend is typical of polar fluorophores that are likely to have enlarged dipoles and charge-transfer character in their excited state.<sup>15</sup> Similar behavior has been observed in related conjugated phenanthrolines.<sup>10</sup> It is important to add that unlike 1,10-phenanthroline, which is essentially nonemissive in water ( $\lambda_{em} = 360$  nm,  $\phi_F \leq 0.01$ ),<sup>16</sup> nucleoside **3** exhibits respectable fluorescence quantum efficiency in aqueous solutions ( $\phi_F = 0.16$ ).<sup>17,18</sup>

Absorption and emission spectra of a singly modified single-stranded oligonucleotide **9** and the corresponding double-stranded DNA duplex **9·10** in an aqueous buffer are shown in Figure 2. The lower energy transitions above ca. 300 nm are practically identical to those of the free nucleoside **3**. In contrast, significant differences are observed in the emission spectra. While the single-stranded oligonucleotide **9** shows a broad emission with a maximum above 400 nm, duplex **9·10** exhibits a shorter wavelength maximum (ca. 385 nm), reminiscent of the emission spectrum of nucleoside **3** in less polar environment (e.g., CH<sub>2</sub>Cl<sub>2</sub>). This observation suggests that the fluorescent nucleoside encounters different environments in the single- vs double-stranded structure.

(14) Removal of the completed oligonucleotides from the solid support using concentrated ammonium hydroxide was followed by incubation at 55 °C for 8–12 h to afford the crude oligonucleotides. The fluorescent oligonucleotides were purified by denaturing polyacrylamide gel electrophoresis and semipreparative HPLC.

(15) Creaser, C. S.; Sodeau J. R. In *Perspective in Modern Chemical Spectroscopy*; Andrews, D. L., Ed.; Springer-Verlag: Berlin, 1990; pp 103–136.

(16) Bandyopadhyay, B. N.; Harriman, A. *J. Chem. Soc., Faraday Trans. 1* **1977**, 73, 663–674.

(17) As expected, the emission quantum efficiency is higher in organic solvents such as acetonitrile ( $\phi_F = 0.22$ ).

(18) Measured in degassed solutions.

To explore whether these emission features can be utilized to follow DNA hybridization, fluorescence-monitored thermal denaturation experiments have been conducted. Figure 4 shows the steady-state emission spectra of duplex **9·10** as

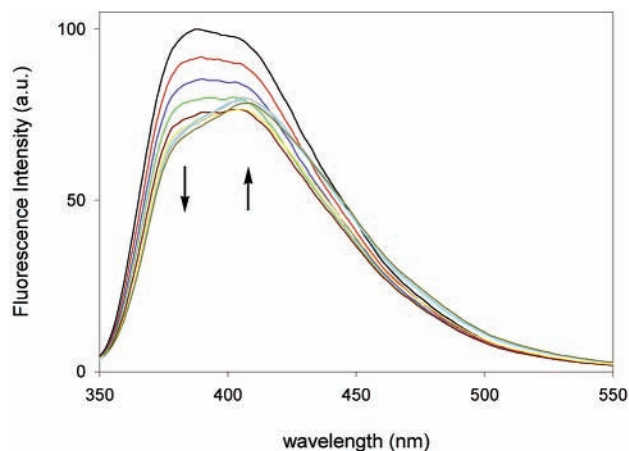


**Figure 4.** Emission spectra of duplex **9·10** as a function of temperature from 35 °C (black) to 75 °C (cyan).

function of temperature. It is apparent that the relative intensity of the species emitting at longer wavelengths increases at elevated temperatures. Plotting the ratio between the intensity of the visible emission at 407 nm (typical of an exposed fluorophore in a single strand) and the shorter emission wavelength at 387 nm (characteristic of a “protected” fluorophore in a less polar duplex environment) yields a denaturation curve that closely follows the melting curve of the duplex as determined by UV absorption spectroscopy (Figure 5). It is important to note that when the fluorescent

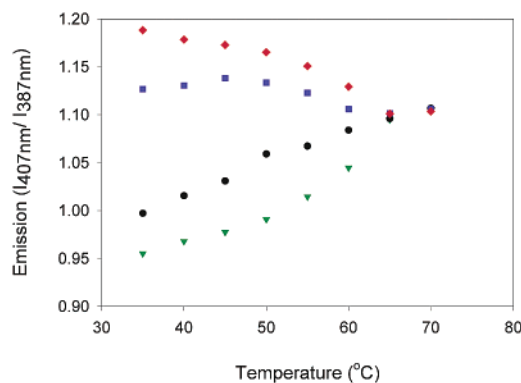


**Figure 5.** Emission-monitored thermal denaturation curves perfect complement **9·10** (green triangle), G mismatch **9·11** (black circle), T mismatch **9·12** (blue square), and C mismatch **9·13** (red diamond).

nucleoside dU<sup>phen</sup> is incorporated at the terminus of a duplex as in **7·8**, the ratio  $I_{407}/I_{387}$  remains unchanged upon

denaturation.<sup>19</sup> We therefore conclude that internally placed dU<sup>phen</sup> residues can be used to monitor duplex formation and denaturation.

To investigate the sensitivity of dU<sup>phen</sup> to the formation of mismatched base pairs, duplexes **9**–**11**–**9**–**13** that contain G, T, or C opposite dU<sup>phen</sup>, respectively, have been assembled. Emission-based thermal denaturation experiments for all DNA sequences are shown in Figure 5. Duplexes containing a single mismatch show higher  $I_{407}/I_{387}$  ratios than the perfect duplex **9**–**10** at ambient temperatures. Interestingly, the emission ratio is sensitive to the nature of the mismatch. Duplex **9**–**11**, containing a reasonably well-tolerated dG–dU<sup>phen</sup> base pair, displays a  $I_{407}/I_{387}$  ratio that is close to that of the native duplex **9**–**10**. In contrast, duplexes containing the destabilizing pyrimidine–pyrimidine pairs (e.g., **9**–**12**, **9**–**13**) exhibit a much higher  $I_{407}/I_{387}$  ratio at ambient temperature. As expected, all curves converge to the same ratio of emission intensity upon thermal denaturation, characteristic of the corresponding single-stranded oligonucleotide **9**. Evidently, the emission-based melting curves of the internally modified dU<sup>phen</sup> duplexes exhibit a distinctive pattern, characteristic of the base opposite the fluorescent base.

A priori, different phenomena can account for the characteristic spectral features and  $I_{407}/I_{387}$  ratios that distinguish the dU<sup>phen</sup>-containing duplexes **9**–**10**–**9**–**13** both from the corresponding modified single strand **9** and from each other: (a) hybridization-induced tautomerization of dU<sup>phen</sup> that alters the electronic nature of the chromophore and thus the spectral features of the single vs the double stranded oligonucleotide, (b) structural perturbation of the duplex upon mismatch formation that disturbs the local environment of dU<sup>phen</sup> thus altering the emission features of the single and double stranded oligonucleotides, and (c) a shift in the equilibrium composition of the double vs the single stranded oligonucleotide. To explore the first possibility, two “trapped tautomers” of dU<sup>phen</sup>, **14** and **15**, have been synthesized and spectrally characterized (Figure 6).<sup>13</sup> As shown in Figure 3, both the *O*-Me derivative **14** and *N*-Me derivative **15** show similar emission energies and sensitivity to solvent polarity when compared to the parent dU<sup>phen</sup>.<sup>14</sup> We therefore exclude the possibility that changes in the  $I_{407}/I_{387}$  ratio are caused by tautomerization of dU<sup>phen</sup> upon hybridization. To investigate the other possibilities, additional emission-based

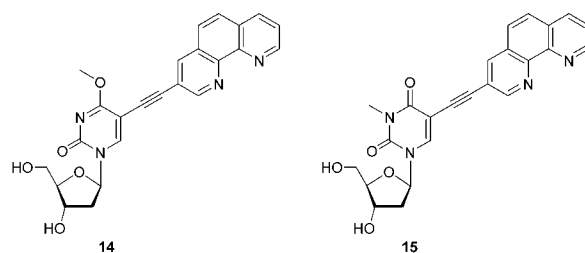


**Figure 6.** Structure of “tautomerically trapped” dU<sup>phen</sup> analogues.

denaturation experiments have been conducted with duplex **9**–**13** and increasing concentrations of the mismatched complement **13**. Although diminished  $I_{407}/I_{387}$  ratios are observed, they never reach the value observed for the perfect duplex, even in the presence of 10-fold excess of complementary oligonucleotide.<sup>13</sup> We therefore conclude that the distinctive  $I_{407}/I_{387}$  ratios observed for mismatched duplexes **9**–**11**–**9**–**13** reflect both a characteristic local environment and a higher equilibrium population of a single stranded structure when compared to the perfect duplex **9**–**10**.

Our results demonstrate that the fluorescent deoxyuridine analogue dU<sup>phen</sup> **3** is a sensitive probe for its local environment within DNA duplexes. Its fluorescence emission as a free nucleoside and within a single-stranded oligonucleotide is different from that observed when incorporated into a DNA duplex. Additionally, the emission-monitored denaturation curves of internally modified dU<sup>phen</sup> duplexes are characteristic of the nucleotide opposite the fluorescent base and allow one to distinguish between the perfect and various mismatched complementary oligonucleotides. It is anticipated that further refinement of the chromophore’s structure may shift the emission wavelengths further into the visible range and may enhance its sensitivity to the local environment.

**Acknowledgment.** We thank the National Institutes of Health (Grant No. GM 58447) for generous support.

**Supporting Information Available:** Synthetic procedures and spectral data for all new derivatives, as well as thermal denaturation and fluorescence spectroscopy experiments. This material is available free of charge via the Internet at <http://pubs.acs.org>.

OL026043X

(19) Since the terminal nucleotide within any duplex is solvent exposed, it does not experience a significant environmental change upon duplex melting. See the Supporting Information.